Available online at www.sciencedirect.com

ScienceDirect

Procedia Engineering 199 (2017) 477–482

Procedia Engineering

www.elsevier.com/locate/procedia

X International Conference on Structural Dynamics, EURODYN 2017

Measurement of rotating beam vibration using optical (DIC) techniques

Ahmed Yashar[a,*], Neil Ferguson[a], Maryam Ghandchi Tehrani[a]

[a]*Institute of Sound and Vibration Research, University of Southampton, Southampton SO17 1BJ, UK*

Abstract

In this paper, an experimental study is presented to validate a dynamic model of a rotating beam. The majority of existing vibration instrumentation is typically wired to an acquisition system through a connection using slip rings. An issue is the inherent signal to noise and the reliability of slip ring electrical connections. Herein, an experimental test rig is designed to overcome these issues. In addition, the rig is conceived to incorporate capabilities such as applying variable rotational speed using a variable frequency driver and provide vertical base excitation input to the centre of the rotation using a linear bearing. The tests are performed using random excitation on the fixed end of the rotating cantilever beam to excite the flapwise modes of the beam. The responses are then measured optically using a single high-speed camera, and the images are post-processed using a digital image correlation (DIC) method. This non-contacting optical method is used to extract the deflection of the beam as a function of time. The frequency response functions are then obtained from the measured responses. The modal frequencies are estimated and compared with numerical simulations to validate a Rayleigh-Ritz and FE numerical model for different rotational speeds.

Peer-review under responsibility of the organizing committee of EURODYN 2017.

Keywords: Rotating beam; Image correlation; Image processing; flapwise vibration;

1. Introduction

Rotating cantilever beams are widely applied in engineering applications, such as in wind turbines, in helicopter blades and in turbomachinery applications. The vibrational characteristics of beams become considerably different when subject to rotation. Numerical approaches to study the phenomena have been widely published [1–3]. However, there are much fewer experimental investigations because of the difficulties in performing the tests. One of the principal obstacles is attaching and connecting instrumentation to the rotating structure. Furthermore, the additional mass of any transducers can also affect the behaviour of the structure. To overcome these issues, in this paper a new digital image processing method is developed to obtain the natural frequencies and final time domain response of a rotating beam. The new non-invasive method is based on measuring the beam deflection optically.

* Ahmed Yashar. Tel.: +44-(0)2380-59-4930-24930 ; fax: +44-(0)2380-59-3190.
E-mail address: amiy1g14@soton.ac.uk

1877-7058
Peer-review under responsibility of the organizing committee of EURODYN 2017.
10.1016/j.proeng.2017.09.052

2. Experimental design

An experimental test rig was designed incorporating a controllable high rotational speed and vertical base excitation. The foundation of the design should be rigid enough to avoid frequency interference between the specimen and the foundation. To achieve these requirements a test rig was designed as shown in Figure 1. This design comprises five main parts. A steel foundation, a high-speed air-cooled controllable motor that provides a speed range between 0-24000 rpm, a variable frequency drive (VFD) to control the rotational speed and a rotational hub.

This design was optimised using vibration analysis in FE. The estimated beam natural frequencies, covering the fundamental, second and third mode are between 8-500Hz and the test rig foundation is about 850Hz, which is much higher than the specimens' frequencies.

The rotating hub assembly allows the introduction of a vertical excitation to the base of the rotational beam as shown in the Figure 2, where the four shafts have the ability to slide in the linear bearings. This vertical excitation was achieved using an electrodynamic shaker, which excites the beam in a flapwise direction at its base.

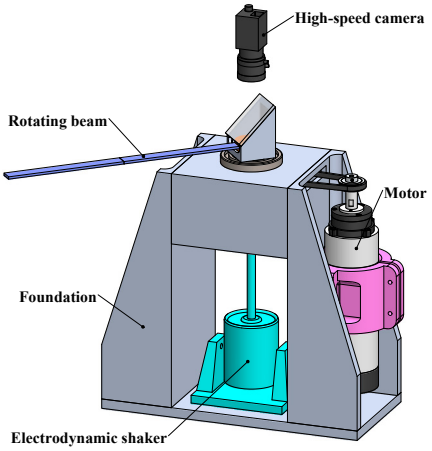

Fig. 1: Experimental test rig with single high speed camera and mirror.

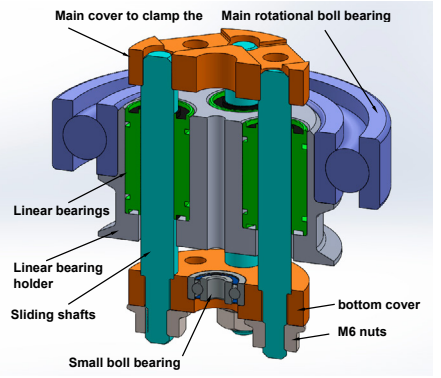

Fig. 2: Section view of rotating hub assembly.

3. Digital image correlation

Digital Image Correlation (DIC) is a pattern tracking method and it is designed to recognise and track a special density of grey levels [4]. To achieve this task, specimen typically are painted with two contrast colours such as black and white as shown in the Figure 3. This pattern should be random and the size of the black points should not be less than three pixels to avoid pixel aliasing. In this paper, three different markers were used instead of the speckles for the purpose of tracking the tags using a simple MATLAB image processing algorithm; a commercial DIC software package was used for comparison with the results. These three markers are a 10mm diameter circle black point, three 2mm diameter black points and five 2mm diameter black points as shown in Figures 3(b)-(d), respectively.

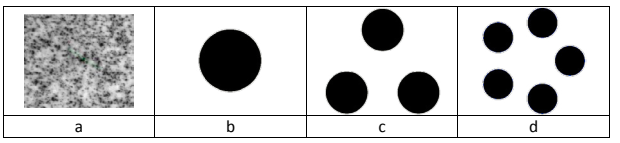

Fig. 3: Illustration of the (a) Speckles and (b-d) Marker patterns.

4. Experimental test setup

4.1. Camera set up methods

The test setup depends on three main aspects; Firstly, the measurement equipment capability (depends on the frame rate and resolution of the sensor for the camera), secondly, the frequency range (depends on the rotation speed and measured frequencies) and third the field test area.

For flapwise vibration of a non-rotating beam, the test configurations shown in Figure 4 are applicable. However, the most suitable arrangement is Figure 4(a), which was previously used for non-rotating beams [5]. A single high-speed camera is set perpendicular to the plane of motion. This arrangement allows the camera to capture the lateral vibration of the beam with minimum equipment.

For the rotating beam the first two setups are difficult to apply. In setup 1 the rotational speed is much lower than the frequencies of the beam. Therefore more than one camera should be used to avoid frequency aliasing. For the second setup, Figure 4(b), the same sampling problem occurs, which requires a high-resolution camera to analyse the field of view. The third and fourth setups Figures 4(c) and 4(d), are contenders for the rotating beam case, because of the continuous capture and minimum field of view area used. The images are also using a rotating frame of reference, which is the same speed as the rotating beam itself.

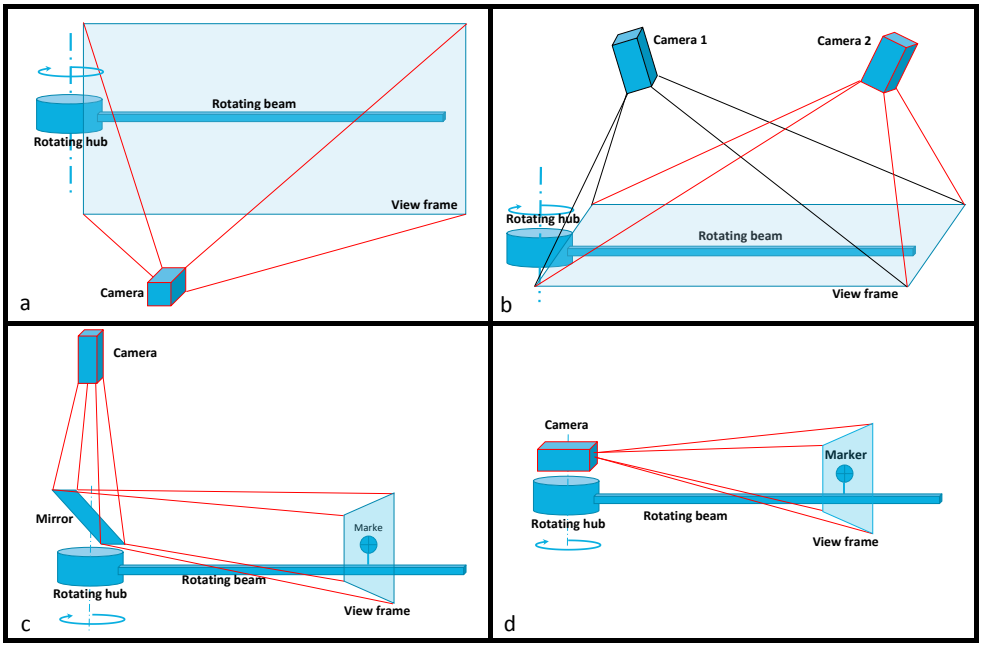

Fig. 4: Types of camera setup: (a) single camera perpendicular to the plane of the lateral displacement, (b) stereo vision system for 3D imaging, two cameras with arbitrary setup angle, (c) single camera with reflecting mirror that targets one or more markers along the beam and (d) single camera fixed to the centre of rotation, targeting one or several markers along the beam.

4.2. Setup for a non-rotating cantilever beam

Experiments were first carried out on a non-rotating beam using DIC to compare the results with the ones obtained using accelerometers. For the DIC system setup, two LED lights are used with a Motion Pro X3 Plus high-speed camera. For the acquisition and recording of the data Motion Studio software was used. On the other hand, the signal system is directly connected to the accelerometer and impact hammer.

In this test, only flapwise or lateral displacement of the beam was measured. For this reason, only one camera is required. The camera is installed perpendicular to the plane of movement. The camera captured the actions in the XY plane when it was fixed in the perpendicular distance Z from this XY plane.

According to the DIC method, the minimum numbers of pixels per black speckle should be at least a 3x3 pixels array in the image. In addition, at least 3 speckles per subset are required to guarantee reasonable matching precision. However, in this experiment the thickness of the beam was 2mm and from equations 1-2. The magnification is also the relationship between the object size on the beam and the image size on the sensor, the equivalent length to the number of the pixels is equal to 2.27 pixels/mm. For this reason a large marker is used instead of a group of speckles as mentioned in Section 3 .

$$Sensor\ size = 1024\ pixels\ number \times 12\mu m\ size\ of\ each\ pixel = 12.288mm \tag{1}$$

$$Magnification = \frac{12.288mm\ Sensor\ size}{450mm\ FOV} = 0.0273 \tag{2}$$

where FOV is field of view.

4.3. Setup for the rotating cantilever beam

Flapwise vibration is out of the rotational plane of motion of the blade. In addition, a rotating beam covers a circular area with a diameter equal to twice that of the rotating beam length and hub radius. This motion can be captured by setting up the high-speed camera perpendicular to the plane of vibration as shown in Figure 4(a). However, this method is limited to being applicable when the maximum vibration frequency to be measured is less than the twice the rotational speed of the beam. The second method uses a stereo vision system. However, a larger area needs a larger number of pixels for accurate measurement. This problem becomes significant when a longer beam is used. Two high-speed cameras capturing the beam from two different angles, then matching of these two images, will reveal the deflection of the beam. Nevertheless, using a single high-speed camera with a reflecting mirror at the centre of rotation solves both aforementioned problems of the sampling rate and image resolution as shown in Figures 4(d) and 4(e).

5. Experimental results

Vibration measurements performed for a non-rotating beam are used for comparison between the results from the image processing methods and the ones obtained from accelerometers. The frequency response function of a non-rotating cantilever beam was measured using a simple impact hammer test. The frequency response function of the non-rotating beam was measured using an accelerometer and the results were compared with simultaneous recordings using a high-speed camera (MotionPro X3 plus, 50mm lens).

MATLAB image processing toolbox was used to locate the displacement of a marker by matching the marker image with the sequence of images. This code recognises dark circular objects and calculates the average distance of each group of circles in the vertical direction. This program is limited to large displacements and therefore the data becomes very noisy for small displacements. However, there are several commercial software packages for DIC, which are able to tackle this issue using the average grey level using subpixels for locating objects. MatchID was employed in this work to postprocess the data. Figure 5 shows the comparsion of results for the three measurement methods namely using an accelerometer (LMS), digital image processing (MATLAB) and digital image correlation (MatchID).

Utilizing two different systems is not efficient due to signal misalignment as well as having different sampling rates between the two systems requiring subsequent data interpolation. This issue was resolved using the same camera to capture both the input signal as well the output. As shown in the block diagram Figure 8, another marker was placed at the centre of rotation. This method is used for random vibration tests to compare between the accelerometers and markers as shown in Figure 6. For the rotating beam, a single camera using a mirror was used to measure the vibration. The reflected image can reveal both the rotational speed and the beam deflection as a function of time. Converting the marker position from the cartesian system to the polar system and by taking the FFT of the time history, the fundamental and second resonance frequencies can be obtained as shown in Figure 9.

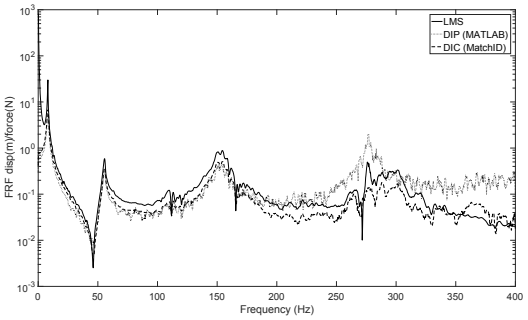

Fig. 5: Comparison between the results from accelerometer LMS, DIP (MATLAB) and DIC (MatchID) methods for specimen No.1 (Beam length=400mm input at 100mm from the fixed end and the output at 300mm from the fixed end). The fundamental natural frequency is 8.14 Hz, second natural frequency is 55.54 Hz and the third natural frequency is 153 Hz.

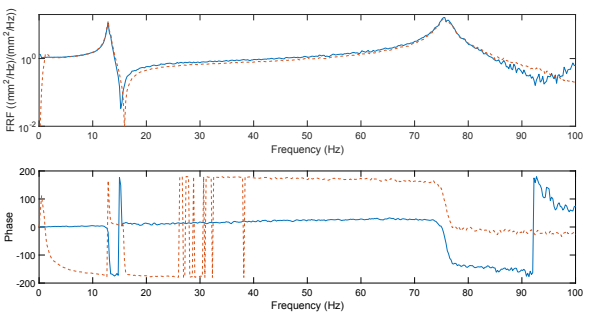

Fig. 6: The measured FRF between the output marker and input marker (blue solid line) and output of the accelerometer and the input marker (red doted line) for the non rotating beam (length=330mm).

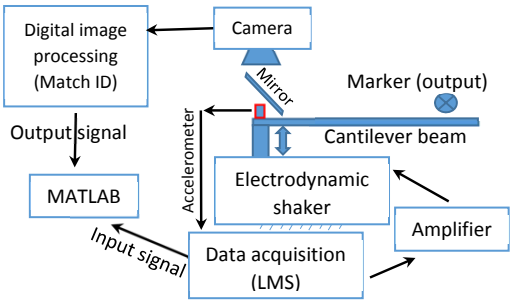

Fig. 7: Experimental test set up

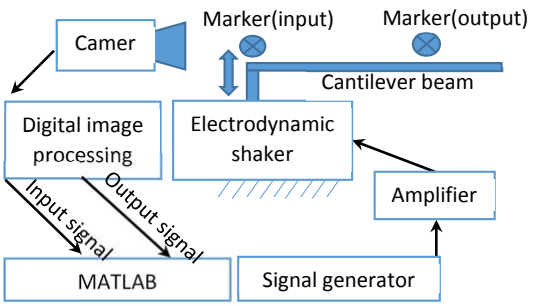

Fig. 8: Experimental test set up

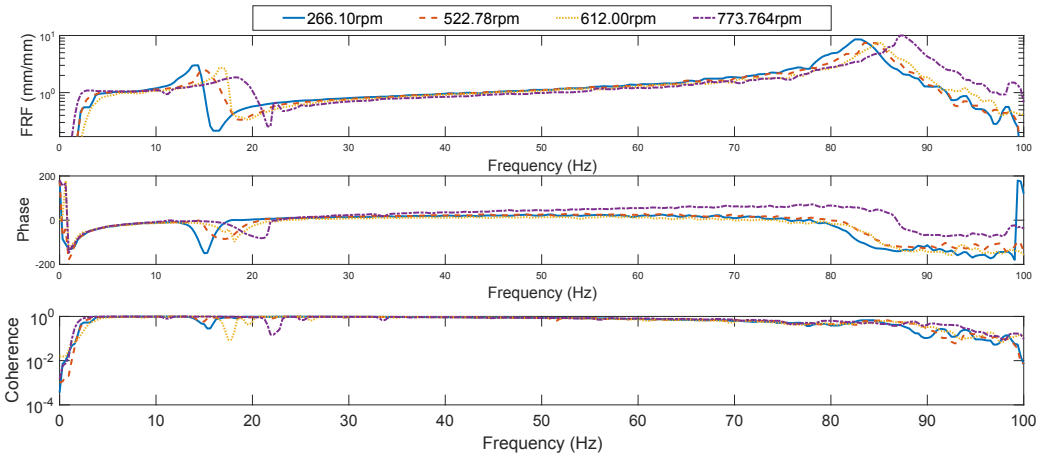

Fig. 9: Frequency response function (transmissibility) of a cantilever aluminium beam with cross section (height=2mm, width=15mm and length=330mm), rotating at different speeds(266, 523, 612 and 773 rpm).

The maximum percentage of the error between the theoretical [6] and experimental results for the first and second resonances are less than 5% as illustrated in Figure 10. The differences between the analytical and the experimentally

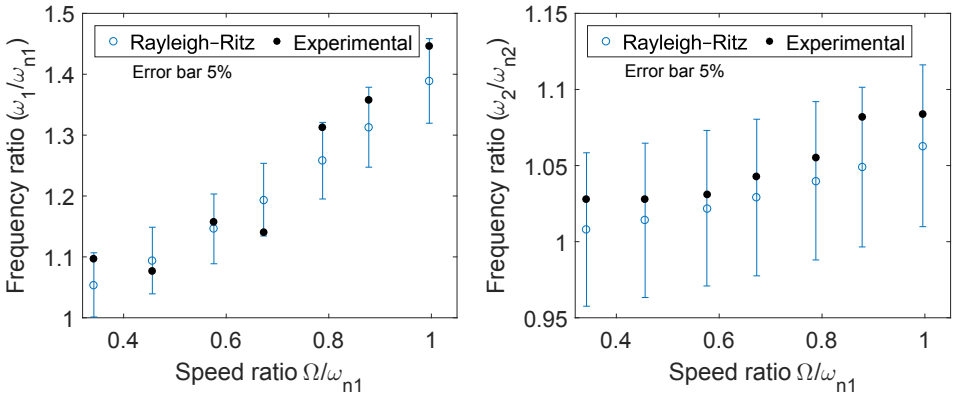

Fig. 10: Comparison of the measured fundamental and second natural frequency of flapwise vibration versus a theoretical model using the Rayleigh-Ritz approach [6]

estimated natural frequencies are partly due to the uncertain boundary conditions in the experimental rig. Theoretically a fixed end was assumed, but where in the experimental test the beam constraint depended upon the clamped edges and applied bolt force. This factor led to a reduction in the estimated frequencies from the experimental results when compared to the theoretical results.

6. Conclusions

In this study, two digital image processing approaches and a typical accelerometer method were used to measure the fundamental and second natural frequencies of a non-rotating beam. Subsequently, the optical approaches were used to determine the first and second resonances of a rotating beam at different rotational speeds.

For a non-rotating beam the results of the hammer and random vibration tests were in a good agreement, particularly at the low frequencies. In addition, for the rotating beam the results showed a gradual rise in the first and second frequencies as the rotational speed increases as predicted in the models previously developed [6]. Furthermore, the digital image processing code showed a good tracking of the beam deflection when the object vibrates at a large amplitude, but the data became noisy when the beam deflection amplitudes were low.

Acknowledgements

The lead author gratefully acknowledges the Ministry of Higher Education and Scientific Research in Iraq for providing full PhD scholarship.

References

[1] J. Chung, H. Yoo, Dynamic Analysis of a Rotating Cantilever Beam By Using the Finite Element Method, Journal of Sound and Vibration 249 (2002) 147–164.
[2] H. H. Yoo, J. E. Cho, J. Chung, Modal analysis and shape optimization of rotating cantilever beams, Journal of Sound and Vibration 290 (2006) 223–241.
[3] H. Kim, H. Hee Yoo, J. Chung, Dynamic model for free vibration and response analysis of rotating beams, Journal of Sound and Vibration 332 (2013) 5917–5928.
[4] M. N. Helfrick, C. Niezrecki, P. Avitabile, T. Schmidt, 3D digital image correlation methods for full-field vibration measurement, Mechanical Systems and Signal Processing 25 (2011) 917–927.
[5] M. Romaszko, B. SapiÅski, A. Sioma, Forced vibrations analysis of a cantilever beam using the vision method, Journal of Theoretical and Applied Mechanics (2015) 243.
[6] A. Yashar, M. Ghandchi-Tehrani, N. S. Ferguson, Dynamic behaviour of a rotating cracked beam, Journal of Physics: Conference Series 744 (2016) 012057.